

Relativistic ionization-rescattering with tailored laser pulses

Michael Klaiber^{1,2,*}, Karen Z. Hatsagortsyan^{1,†} and Christoph H. Keitel^{1,‡}

¹*Max-Planck Institut für Kernphysik, Saupfercheckweg 1, D-69117 Heidelberg, Germany*

²*Theoretische Quantendynamik, Physikalisches Institut der Albert-Ludwigs-Universität, Hermann-Herder-Straße 3, D-79104, Freiburg, Germany*

(Dated: February 2, 2022)

The interaction of relativistically strong tailored laser pulses with an atomic system is considered. Due to a special tailoring of the laser pulse, the suppression of the relativistic drift of the ionized electron and a dramatic enhancement of the rescattering probability is shown to be achievable. The high harmonic generation rate in the relativistic regime is calculated and shown to be increased by several orders of magnitude compared to the case of conventional laser pulses. The energies of the revisiting electron at the atomic core can approach the MeV domain, thus rendering hard x-ray harmonics and nuclear reactions with single atoms feasible.

PACS numbers: 42.65.Ky, 32.80.Gc, 32.80.Rm

In intense laser-atom interaction phenomena the rescattering concept plays a central role [1]. Here the electron is ionized, propagated in the continuum by the laser field, and finally driven back and scattered at the ionic core in the case of above-threshold ionization (ATI)[2], ionizing further bound electrons in the case of non-sequential double ionization (NSDI) [3], or recombining with the ionic core with high-harmonic generation (HHG) [4]. It is highly desirable to increase the rescattering electron energy [5] as it can be employed to generate higher harmonics [6], to image attosecond dynamics of nuclear processes [7], or to initiate nuclear reactions with a single atom/molecule [8, 9]. The electron energy increase can not be achieved by a straightforward increase of the laser intensity. When the laser intensity approaches the relativistic regime, the laser magnetic field effect starts to play a role by inducing a drift of the ionized electron in the laser propagation direction which severely suppresses the probability of the electron revisiting the ionic core. There are several attempts to circumvent this effect in order to increase the efficiency of rescattering, particularly, using relativistic ions which propagate in laser propagation direction [6, 8], or using two counter-propagating laser beams with linear [10] or equally handed circular polarization [7], or generating harmonics via exotic positronium atoms in strong laser fields [11]. On a different front, new techniques for generating attosecond pulses have recently emerged based on HHG in gases [12, 13] and in plasmas interaction [14, 15]. The usage of attosecond pulse trains (APT's) to enhance HHG in a strong laser field has been shown in [16].

In this letter we show how efficient recollisions in the relativistic regime are feasible by employing specially tailored strong laser pulses in the form of APT's (see Fig.1). As an indicator of strong field recollision phenomena we consider the HHG process from an ion in a relativistically strong tailored laser pulse (see Fig.2). While in [16] the weak APT serves to solely control the initial conditions of the ionized electron in the strong laser field, we consider

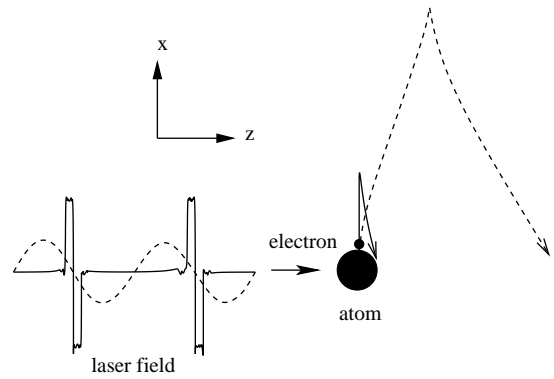


FIG. 1: By using optimized tailored pulses in the form of an APT instead of conventional sinusoidal pulses it is possible to reduce significantly the drift of the ionized electrons due to the Lorentz force of the laser field (the ionized electron trajectory in the sinusoidal pulse is shown as a dashed line, in the tailored pulse as a solid line). Therefore, the rescattering probability can be increased by several orders of magnitude in the relativistic regime of laser-atom interactions. x and z are the laser polarization and propagation directions, respectively.

HHG in relativistically strong APT. The temporal tailoring of the laser pulse is aimed to concentrate the ionizing and afterwards the accelerating laser forces in short time intervals within the laser period (maintaining the average intensity of the pulse constant) which substantially reduces the relativistic drift. This results from the fact that in the tailored laser pulse, fragments in the electron trajectory are avoided, in contrast to the sinusoidal laser pulse, in which the electron acceleration is compensated by deceleration without a net energy gain by the electron, but during which nevertheless the electron would continue to drift in the laser propagation direction (see Fig. 3(ii)). This substantially decreases the time span during which the electron moves with a relativistic velocity. The latter results in a shorter drift in the laser

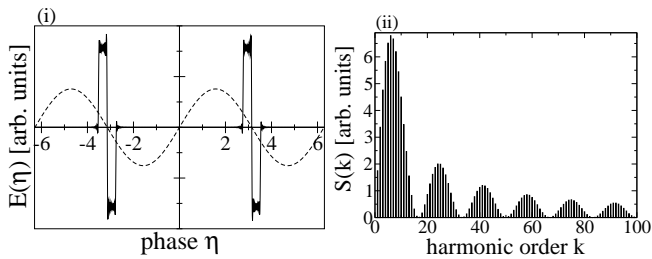


FIG. 2: The tailored laser pulse in the form of an APT, with each pulse duration in the train being $\tau = 0.12\pi$ a.u.: (i) Phase dependence of the electric field ($E(\eta)$) of the tailored pulse (solid line) compared with a sinusoidal field (dashed line) with equal average intensities and central angular frequency $\omega = 0.1$ a.u.; (ii) Frequency spectrum ($S(k)$) of the tailored pulse. The frequency components are phase locked.

propagation direction, and therefore, in an increase of the recombination probability in the case of the tailored pulse.

The scenario of the electron motion in the tailored laser pulse looks as follows. The trajectory of the rescattering electron begins at the end of the period with maximal field strength of the laser pulse, shortly before the field free region. The initial spike of the laser pulse ionizes the electron and initiates its excursion with a very low initial velocity. The acceleration of the electron takes place during the next spike after the field free region. One can see from Fig. 3 that in the tailored wave the electron gains most of its energy only shortly before the recombination and the trajectory of the electron in the tailored pulse is spatially significantly shorter than in the sinusoidal wave.

The procedure for tailoring the laser pulse is the following. The laser pulse with temporal form as shown in Fig.2 has been chosen with the additional condition of vanishing the field average of the pulse $\langle E \rangle = 0$. Then, the

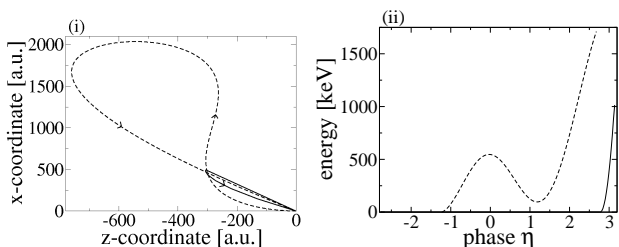


FIG. 3: Trajectory and kinetic energy of an HHG electron in the tailored wave (solid line) and in a sinusoidal wave (dashed line) with an averaged laser intensity of 5×10^{19} W/cm². (x and z are the polarization and propagation direction of the laser field, respectively.) The electron is ionized at a phase of -1.24 in the sinus wave and recombines at a phase of 2.68 . In the tailored wave the electron is ionized at a phase of -2.78 and recombines at a phase of 3.14 .

Fourier-expansion of this pulse is used via $K = 100$ harmonic terms to optimize the field expansion coefficients by maximizing the rescattering (HHG) probability. The optimized tailored pulse has the form of an APT which includes three key features. The first is a large ionization peak with a strong decay after the point of ionization (the stronger decay the larger HHG efficiency). This follows by a long region with an only weak field strength (the longer the better) which is resumed by a short and strong pulse that induces most of the energy of the ionized electron. The optimized pulse along with its spectrum is shown in Fig. 2. The rescattering rate resulting from this pulse can be enhanced by using more frequency components in the APT. In the calculated spectra that will follow, we employ 100 frequency components. When using only $K = 30$ harmonics in the tailored pulse, the HHG yield decreases by approximately 2 orders of magnitude at laser intensity of 5×10^{18} W/cm² and by 5 orders of magnitude for 5×10^{19} W/cm². A possible experimental way for the above mentioned tailoring of the laser pulses is to employ relativistic harmonics generated during a laser-foil interaction in the so-called sliding mirror regime [15] which yields very strong APT's with a conversion efficiency of a few percent. Additionally the technique for the spectral filtering [12] should be applied to form the necessary spectral dips as shown in Fig. 2. Significantly less spectral filtering would be necessary when using $K = 30$ harmonics and a APT spectrum with one hump, though in this case the HHG yield will be reduced as indicated above.

Given the tailored laser pulse, we proceed to calculate the HHG intensity. Our investigation of HHG in an optimized tailored laser pulse is based on the solution of the Klein-Gordon equation in the strong field approximation (SFA) [17]. We consider the HHG process of an atomic system by a linearly polarized plane laser field for the relativistic parameter regime. The direction of the laser field polarization is along the x axis, that of the magnetic field along the y , and of the laser propagation along the z axis. The amplitude of HHG within the SFA based on the Klein-Gordon equation in the single-active electron approximation is given by the following expression [18] (atomic units are used throughout the paper):

$$M_n = -i \int d^4x' \int d^4x'' \{ \Phi(x')^* \times V_H(x') G^V(x', x'') V_A(x'') \Phi(x'') \} \quad (1)$$

with n the harmonic order, Φ the bound state wave function, $V_H(x) = 2\mathbf{A}_H(x) \cdot (\hat{\mathbf{p}} + \mathbf{A}(\eta))/c$, $V_A(x) = 2iV(x)/c^2\partial_t + V(x)^2/c^2$, $V(x)$ the atomic potential, c the speed of light, $\hat{\mathbf{p}}$ the momentum operator of the electron, $\mathbf{A}(\eta)$ the vector potential of the laser field in the radiation gauge, $k^\mu = (\omega/c, 0, 0, k)$ its 4-wavevector, $\eta = k^\mu x_\mu$, $x^\mu = (ct, \mathbf{x})$ the time-space coordinate, $\mathbf{A}_H(x)$ the matrix element of the vector potential of

the high harmonic field in the second quantization for an one photon emission process, and $G^V(x', x'')$ the Klein-Gordon Volkov Green function given in Ref. [18]. Φ is an eigenstate of the physical energy operator in the radiation gauge and can be approximated as $\Phi(x) = \phi_0(\mathbf{x}) \exp\{-i[(c^2 - I_p)t + \mathbf{x} \cdot \mathbf{A}/c]\} / \sqrt{2(c^2 - I_p)}$ [19], with the nonrelativistic ground state wave function $\phi_0(\mathbf{x})$. Introducing the integration variable transformations $\eta' = k^\mu x'_\mu$ and $\eta'' = k^\mu x''_\mu$ and taking into account that the atomic wave function characteristic length is much smaller than the laser wavelength, the amplitude of HHG can be written:

$$M_n = \int_{-\infty}^{\infty} d\eta' \int_{-\infty}^{\eta'} d\eta'' \int d^3\mathbf{q} m^H(\mathbf{q}, \eta', \eta'') \times \exp\{-i[S(\mathbf{q}, \eta', \eta'') - n\eta']\} \quad (2)$$

with the HHG matrix element for emission in laser polarization direction

$$m^H(\mathbf{p}, \eta', \eta'') = -\frac{c^2(p_x + A(\eta')/c)}{\varepsilon_{\mathbf{p}}\omega^2} \times \tilde{\phi}_0^* \left(\mathbf{p} + \frac{\mathbf{A}(\eta')}{c} - \frac{\mathbf{k}}{\omega}(\varepsilon_{\mathbf{p}} + I_p - c^2) \right) \times \left\langle \mathbf{p} + \frac{\mathbf{A}(\eta')}{c} - \frac{\mathbf{k}}{\omega}(\varepsilon_{\mathbf{p}} + I_p - c^2) | V | 0 \right\rangle, \quad (3)$$

with the Fourier transform of the ground state wave function $\tilde{\phi}_0$ and $\varepsilon_{\mathbf{p}} = \sqrt{c^4 + c^2\mathbf{p}^2}$. $S(\mathbf{p}, \eta, \eta') = \int_{\eta'}^{\eta} d\tilde{\eta} (\tilde{\varepsilon}_{\mathbf{p}}(\tilde{\eta}) - c^2 + I_p) / \omega$ is the quasi-classical action and the relativistic energy is given by

$$\tilde{\varepsilon}_{\mathbf{p}}(\eta) = \varepsilon_{\mathbf{p}} + \frac{\omega}{k \cdot \mathbf{p}} (\mathbf{p} + \mathbf{A}(\eta)/2c) \cdot \mathbf{A}(\eta)/c. \quad (4)$$

The differential rate of HHG is then given by

$$\frac{dw_n}{d\Omega} = \frac{\omega^2}{(2\pi)^3} \frac{n\omega}{c^3} |M_n|^2 \quad (5)$$

with the solid angle of emission Ω .

Using the low-frequency approximation $K\omega \ll I_p$ with the ionization potential I_p , the integral in Eq.(2) can be calculated via the saddle-point method. The saddle point conditions along with the cutoff condition determine the ionization and recombination phases $\tilde{\eta}'$, $\tilde{\eta}''$, as well as the cutoff harmonic number \tilde{n} :

$$\begin{aligned} \tilde{\varepsilon}_{\tilde{\mathbf{q}}}(\eta') &= c^2 - I_p + n\omega \\ \tilde{\varepsilon}_{\tilde{\mathbf{q}}}(\eta'') &= c^2 - I_p \\ \frac{d\tilde{\varepsilon}_{\tilde{\mathbf{q}}}(\eta')}{d\eta'} &= 0, \end{aligned} \quad (6)$$

with the drift momentum of the ionized electron $\tilde{q}_x = -\frac{\int_{\tilde{\eta}''}^{\tilde{\eta}'} d\tilde{\eta} A(\tilde{\eta})/c}{\tilde{\eta}' - \tilde{\eta}''}$, $\tilde{q}_y = 0$, $\tilde{q}_z = \frac{\tilde{q}_x^2 + q_m^2/2}{\sqrt{c^2 - q_m^2 - \tilde{q}_x^2}}$, with $q_m^2 = -(1/c^2) \int_{\tilde{\eta}''}^{\tilde{\eta}'} d\tilde{\eta} \mathbf{A}(\tilde{\eta})^2 / (\tilde{\eta}' - \tilde{\eta}'')$ [18]. In tailoring the laser

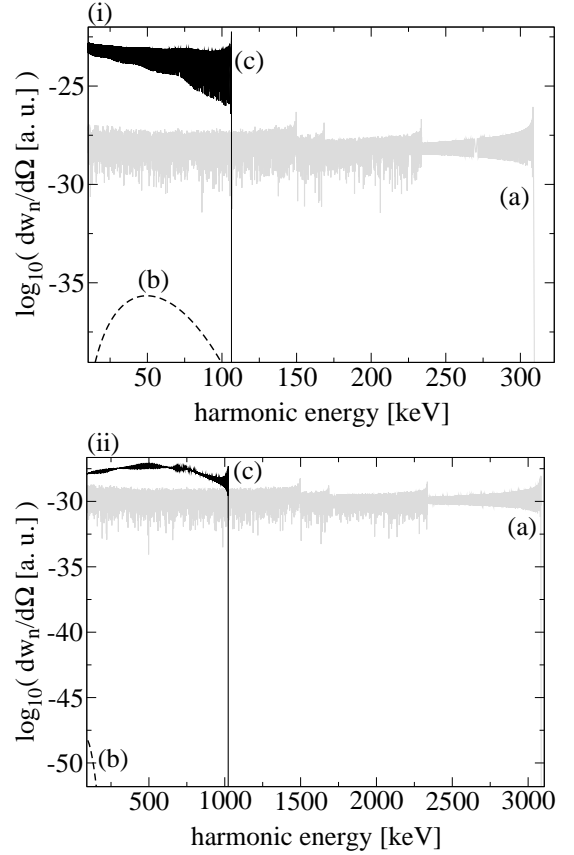


FIG. 4: Harmonic emission rate in laser polarization direction via $\log_{10}(dw_n/d\Omega)$ in Eq. (5), as function of the harmonic energy with a laser intensity of (i) 5×10^{18} W/cm² and (ii) 5×10^{19} W/cm². The main angular frequency is $\omega = 0.1$ a.u.. The ionization potential is (i) $I_p = 28$ a.u. and (ii) $I_p = 62$ a.u., respectively: (a, grey) within the dipole approximation and a sinusoidal field, (b, dashed) with respect to the Klein-Gordon equation and a sinusoidal field, (c, black) with respect to the Klein-Gordon equation and a tailored pulse.

pulse, we fix the harmonic cutoff \tilde{n} and by changing the shape of the pulse, minimize the imaginary part of the ionization time $\text{Im}\{\tilde{\eta}''\}$ which determines the plateau height and, therefore, the rescattering efficiency. Further, the atomic potential $V(x)$ is approximated by a zero-range potential [20]. The ionization potential I_p is adapted to the threshold of the barrier suppression ionization model.

The HHG spectrum with the tailored pulse is compared with two calculations for the harmonic emission using a sinusoidal field. While the first calculation is based on the dipole approximation (DA), the second one is fully-relativistic. We consider two regimes: the moderately relativistic regime with a laser intensity of the tailored pulse 5×10^{18} W/cm² and the strongly relativistic regime with a laser intensity of 5×10^{19} W/cm², each with a laser ground angular frequency of 0.1 a.u., correspond-

ing to a laser wavelength of $\lambda = 456$ nm. Taking into account a few percent efficiency in the APT generation via laser-foil interaction [15], as well as about 20% intensity reduction because of spectral filtering in the case of $K = 100$ spectral components in APT, the initial laser intensity before tailoring should be three orders of magnitude larger. For pulses involving fewer high harmonics this loss may be reduced.

In the moderately relativistic regime (see Fig.4(i)), the harmonic emission rate with conventional laser field is suppressed by over seven orders of magnitude in the relativistic treatment compared with the results in the DA. Whereas the tailored pulse yields a harmonic emission rate that is nearly four orders of magnitude higher than the rate in the dipole approximation. Further the spectrum induced by the tailored pulse as well as the spectrum induced by the sinusoidal field using the DA is highly oscillating, resulting from interference of at least two trajectories of the ionized electron. In the case of the tailored pulse, there are exactly two, since the trajectories with multiple return to the ionic core are very unlikely.

The HHG spectrum in the strong relativistic regime with a laser intensity of 5×10^{19} W/cm² is shown in Fig. 4(ii). Whereas the tailored pulse spectrum is still more intense than the spectrum in the DA with a conventional laser field, the relativistic treatment of HHG with sinusoidal fields yields a rate that is negligibly small. From the HHG spectrum one can see that cutoff energies of more than 1 MeV are reachable with the probability not less than in the DA.

The enhancement of the HHG rate via tailored pulses compared with the one via a sinusoidal field is due to the suppressed relativistic drift. This can be deduced by comparing the trajectory of the ionized cutoff electron driven by the tailored pulse with one driven by the sinusoidal pulse, see Fig. 3(i). The excursion of the ionized electron in polarization and propagation direction in the tailored pulse is shorter, though the averaged intensity of the pulses are the same. Moreover, the HHG emission angle with respect to the laser polarization direction in the tailored pulse is significantly smaller than in the conventional sinusoidal field (see Fig. 3(i)). In other terms, the suppressed drift can be deduced by the value of initial electron velocity in the laser propagation direction, necessary for the electron rescattering in the relativistic regime. In the tailored pulse it is much smaller compared to that for a sinusoidal pulse. In fact, in the strongly relativistic regime, the numerical values for the initial velocity in the tailored pulse is -6 a.u., whereas for the sinusoidal field -97 a.u.. The initial velocity of the tunneled electron determines the exponential damping factor of the electron tunneling probability, yielding a higher ionization rate and, therefore, a higher HHG efficiency, in the tailored pulse as compared to the sinusoidal field.

The reason for the increased HHG rate with the tai-

lored laser pulse over the dipole approximation rate is that the laser electric field strength at the time of ionization is higher in the tailored pulse at the same average laser intensity. The numerical values are $|E(\tilde{\eta}'')| = 74$ a.u. for the tailored pulse and $|E(\tilde{\eta}'')| = 36$ a.u. for the sinusoidal field for a laser intensity of 5×10^{19} W/cm².

Further, one can make a statement about the stability of the HHG process driven by such a tailored laser pulse. A random variation of the amplitude of the frequency components by 5 percent, and of the phases within the range not exceeding $\pi/100$, results in a variation of the HHG yield within one order of magnitude.

Concluding, employing specially tailored laser pulses in the form of an APT allows to suppress the relativistic drift of the ionized electron and to realize ionization-rescattering in the relativistic regime. HHG in the hard x-ray domain and the initiation of nuclear reactions with single ions thus become feasible.

Funding by Deutsche Forschungsgesellschaft via KE-721-1 is acknowledged.

* Electronic address: klaiber@mpi-hd.mpg.de

† Electronic address: k.hatsagortsyan@mpi-hd.mpg.de

‡ Electronic address: keitel@mpi-hd.mpg.de

- [1] P. B. Corkum, Phys. Rev. Lett. **71**, 1994 (1993).
- [2] P. Agostini *et al.*, Phys. Rev. Lett. **42**, 1127 (1979); P. H. Bucksbaum *et al.*, Phys. Rev. Lett. **56**, 2590 (1986); G. G. Paulus *et al.*, Phys. Rev. Lett. **72**, 2851 (1994).
- [3] S. Augst *et al.*, J. Opt. Soc. Am. B **8**, 858, 1991; B. Walker *et al.*, Phys. Rev. A **48**, R894, 1993.
- [4] A. McPherson *et al.*, J. Opt. Soc. Am. B **4** 595 (1987); M. Ferray *et al.*, J. Phys. B **21** L31 (1988).
- [5] Y. I. Salamin, *et al.*, Phys. Rep. **427**, 42 (2006).
- [6] C. C. Chirila *et al.*, Phys. Rev. Lett. **93**, 243603 (2004).
- [7] N. Milosevic, P.B. Corkum, and T. Brabec, Phys. Rev. Lett. **92**, 013002 (2004).
- [8] G. Mocken, and C. H. Keitel, J. Phys. B **37**, L275 (2004).
- [9] S. Chelkowski, A. D. Bandrauk, and P.B. Corkum, Phys. Rev. Lett. **93**, 083602 (2004).
- [10] N. Kylstra *et al.*, Phys. Rev. Lett. **85**, 1835 (2000).
- [11] B. Henrich, K. Z. Hatsagortsyan and C.H. Keitel, Phys. Rev. Lett. **93**, 013601 (2004).
- [12] P. M. Paul *et al.*, Science **292**, 1689 (2001); Y. Mairesse, *et al.*, Science **302**, 1540 (2003); R. Lopez-Martens *et al.*, Phys. Rev. Lett. **94**, 033001 (2005).
- [13] M. Hentschel *et al.*, Nature **414**, 509 (2001); P. Tzallas *et al.*, *ibid.* **426**, 267 (2004); R. Kienberger *et al.*, *ibid.* **427**, 817 (2004).
- [14] N. M. Naumova, Phys. Rev. Lett. **92**, 063902 (2004); S. Gordienko, *et al.*, Phys. Rev. Lett. **93**, 115002 (2004).
- [15] A. S. Pirozhkov *et al.*, Phys. Plasmas **13**, 013107 (2006).
- [16] K. Schafer *et al.*, Phys. Rev. Lett. **92**, 023003 (2004); Phys. Rev. A **72**, 013411 (2005).
- [17] L. V. Keldysh, Sov. JETP **20**, 1307 (1964); F. H. M. Faisal, J. Phys. B **6**, L89 (1973); H. Reiss, Phys. Rev. A **22**, 1786 (1980); *ibid.* **42**, 1476 (1990); J. Opt. Soc. Am. B **7**, 574 (1990).

- [18] D. B. Milosevic, S. X. Hu, and W. Becker, Phys. Rev. A **63**, 011403 (2000); Laser Phys. **12**, 389 (2002).
- [19] M. Klaiber, K. Z. Hatsagortsyan, C. H. Keitel, Phys. Rev. A **73**, 053411 (2006).
- [20] W. Becker *et al.*, Adv. At. Mol. Opt. Phys. **48**, 35 (2001).